



Optimal Filter Length Selection for Universal Filtered Multicarrier Systems

R. Manda^{*a}, A. Kumar^a, R. Gowri^b

^aDepartment of Electrical and Electronics Engineering, School of Engineering, University of Petroleum & Energy Studies, Dehradun, India

^bDepartment of Electronics and Communication Engineering, Graphic Era Hill University, Dehradun, India

PAPER INFO

Paper history:

Received 06 October 2022

Received in revised form 03 April 2023

Accepted 04 April 2023

Keywords:

Bit Error Rate

Finite Impulse Response

Inter Carrier Interference

Inter Sub-band Interference

Signal to Interference Ratio

Universal Filtered Multi-carrier

ABSTRACT

Future wireless networks will use Universal Filtered Multicarrier (UFMC) as a new waveform modulation technique. The UFMC waveform sensibly considers the sub-band filter specifications such as filter order, and shape to combine the key benefits of the present generation modulation waveforms while averting their disadvantages. Therefore, in UFMC-based systems, it is important to pay attention to how the sub-band filter is made. In this paper, the sub-band filter configuration is adapted according to the sub-band size such that the UFMC symbol generates the minimum level of interference with minimum frequency selectivity. Also, the total interference caused by inter-carrier interference (ICI) and inter-sub-band interference (ISBI) was studied by finding the closed form of its change in the UFMC signal with sub-band size and filter length. From this analysis, we determined the ICI increases and ISBI decreases with filter length. Therefore, the proposed method optimizes the filter length in terms of sub-band size and interference. By this approach, the filter length is shorter than the conventional method and hence improves the symbol utilization. With the proposed method, the overall signal-to-interference ratio (SIR) improved by 1 to 3 dB.

doi: 10.5829/ije.2023.36.07a.13

1. INTRODUCTION

The fast growth in smart terminals, real-time interactive services, and the internet of everything (IoE) inspired the evolution of fifth generation (5G) networks. The key technical challenges for realizing this future network include the physical layer transmission techniques that are required to support efficient spectrum utilization to get full data rate, lower system implementation complexity, lower out-of-band emission (OBE) to minimize the interference, ultra-low latency, and artificial intelligence (AI) based estimation algorithms [1-3]. In the present broadband wireless system, Orthogonal Frequency Division Multiplexing (OFDM) is one of the most frequently used modulation waveforms. However, OFDM has several weaknesses, such as large sidelobes, high bandwidth usage, and severe synchronization requirements, which makes it ineffective for 5G and beyond. For wide-area IoT applications, the communication link must support in-depth coverage, low power consumption, and low implementation complexity

[4]. These limitations enforce to design of a new and flexible modulation waveform that needs to support asynchronous transmission, lower side lobes, and reduced latency with less baseband system complexity [5-9]. In the last few years, several waveform candidates such as Generalized Frequency Division Multiplexing (GFDM) [10], Filter Bank Multicarrier (FBMC) [11], Filtered OFDM [12], and UFMC [13] have been proposed for next-generation wireless systems with a lower OBE. Among them, the UFMC waveform is the most recommended candidate waveform in the 5G and beyond 5G wireless systems to meet the main key performance parameters such as lower OBE, flexible packet transmission, and highly suitable for short packet transmission [14, 15].

The UFMC waveform is a combined form of FBMC and F-OFDM, in which, a group of subcarriers (SCs) is filtered individually to make it more robust in relaxed synchronization conditions compared to OFDM. The sub-band filtering can be physical resource block (PRB) based, service-based, and user-based [16, 17]. The

*Corresponding Author Institutional Email: rajaec6405@gmail.com
(R. Manda)

UFMC is suitable for PRB-based sub-band filtering and massive machine-type communications. In case of the multi-service or multi-user approach the signaling overhead may save but the sub-band filtering disrupts the orthogonality between the subcarriers and introduces inter-carrier interference (ICI) and inter-sub band/service interference (ISBI). In addition, the UFMC system has a higher baseband complexity and computation complexity than traditional OFDM because of the quantity of IFFT blocks and sub-band filters. This computational complexity reduced with different approaches like simplified the baseband UFMC symbol to reduce the number of arithmetic operations discussed in literature [18-22]. Like a cyclic prefix (CP) in OFDM, the subband filter protects against multipath fading and inter-symbol interference (ISI) in the UFMC system. However, on both sides of the symbol, the ramp (filter tail) of the sub-band filter causes interference on neighboring sub-bands, which depends on the filter length. In practice, the sub-band filter length is preferred longer or equal to the wireless channel length to avoid the multipath fading effect [13]. But, in some scenarios, the short filter length can be sufficient to get marginal system performance, which means further the system overhead can be reduced reasonably.

Recently, there are several filter optimization and baseband signal processing approaches have been proposed to mitigate the interference in the UFMC system [23-29]. Mukherjee et al. [23], Wang et al. [30] optimized the sub-band FIR filter based on the knowledge of expected timing offset and frequency offset to reduce the out-band radiation and hence reduced the ISBI. In this method of approach, the filter is fixed and chosen arbitrary without knowledge of the adjacent sub-bands. The active interference cancellation approach is suggested by Zhang et al. [24] uses a separate subcarrier on either side of the sub-band for interference cancellation and optimizing their weights within the power constraints to maximize the overall signal-to-interference ratio (SIR). With this approach, the spectral efficiency degraded due to the use of dedicated subcarriers to cancel interference. An adaptive modulation and filter configuration was proposed by Chen et al. [25], which adaptively determined the sub-band filter impulse response parameters to reduce the interference caused by carrier frequency offset (CFO). This method used some guard band between adjacent sub-bands that causes reduction in spectral usage with better BER performance compared to the conventional method.

From the above literature, all the methods optimized the filter configuration to reduce the interference due to out of band emission, CFO and timing offset. some of these methods used extra subcarrier or guard interval, because of this the symbol utilization degraded. In this article, the filter length is adapted according to the sub-

band width to minimize interference without degrading the symbol utilization. Additionally, we derived the closed form for the interference in the UFMC symbol due to filtering operation and then optimize the filter length for sub-band size. Here, each user's sub-carriers (sub-band size) allocation is determined by the service they seek, such as data, streaming video, or online interactive gaming. As a result, each sub-band has a different length and the correspondingly filter length varies. Here, the proposed method does not use any guard interval between adjacent sub-band. Consequently, the sub-band filter performs fewer calculations, increasing the symbol utilization ratio.

Following are the remaining sections of the paper: The discussion of the UFMC transmitter model and its symbol model is given in section 2. Concerning the filter length and sub-band size, Section 3 focuses on the analysis of ISBI and ICI fluctuation and covers the computation of filter parameters for 5G-NR numerology. Section 4 covers the results and discussion section, and the performance comparison of the UFMC system. Section 5 is devoted to conclusion.

2. UFMC WAVEFORM MODEL

An overview of the UFMC system model can be seen in Figure 1. The basic principle of the UFMC modulator is to divide the total number of data subcarriers N_{DC} (bandwidth) into a group of consecutive subcarriers (known as sub-band), a specific constellation modulated (Quadrature Amplitude Modulation (QAM)) data samples allocated to each sub-band and then performed N-point IFFT after subcarrier mapping on a total number of subcarriers (N) and zeros padded to the unallocated subcarriers. These time-domain sub-band signals are filtered individually with an FIR filter and summed to generate the UFMC signal. In the case of a multi-service/user-based communication system, multiple PRBs allocated to each user or service are considered sub-band.

Consider the UFMC system with B sub-bands and Q_p subcarriers in each sub-band i.e., $\sum_{p=0}^{B-1} Q_p = N_{DC}$; $p = 0, 1, \dots, B-1$. The result of the subband filtering operation, which is the linear convolution of the sub-band signal $s_p(n)$ and the impulse response of the subband filter $f_p(n)$.

$$x_p(n) = \sum_{l=0}^{L_f-1} f_p(l) s_p(n-l) = 0, 1, \dots, N + L_f - 2 \quad (1)$$

It is possible to express the final UFMC signal as:

$$x(n) = \sum_{p=0}^{B-1} \sum_{l=0}^{L_f-1} f_p(l) s_p(n-l) \quad (2)$$

where L_f is the subband FIR filter length, $f_p(l)$ represents the filter impulse response of p^{th} sub-band, which is the center frequency shifted of the prototype filter impulse response ($f(l)$) corresponding to the sub-band. That is:

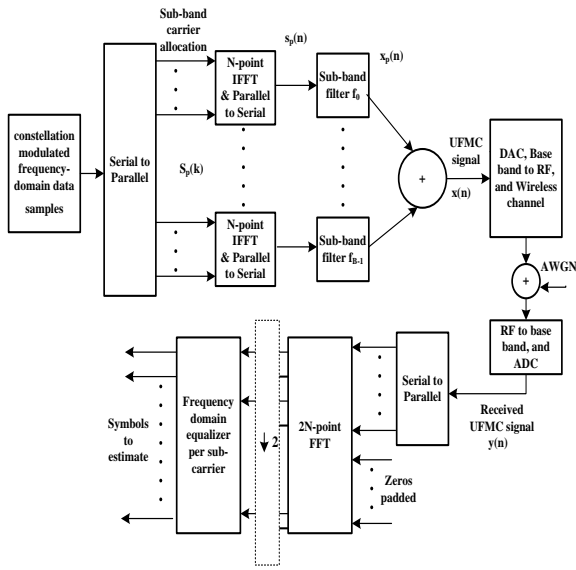


Figure 1. The UPMC system model

$$f_p(l) = f(l)e^{j\frac{2\pi}{N}(K_0+K_p\text{shift})l} ; l = 0, 1, \dots, L_f - 1 \quad (3)$$

where, $K_{p\text{shift}} = \sum_{b=0}^{p-1} Q_b + Q_p/2$; $K_0 = \frac{N-N_{DC}}{2}$ signifies the beginning subcarrier index of the lowest possible sub-band of the UPMC signal. Generally, the filter length for a different sub-band is not necessarily the same. The time-domain sub-band signal $s_p(n)$ represents the N-point IFFT of p^{th} sub-band written as:

$$s_p(n) = \frac{1}{N} \sum_{k=0}^{Q_p-1} S_p(k) e^{j\frac{2\pi}{N}(K_0+K_p+k)n} \quad (4)$$

where the sequence $S_p(k)$ represents the p^{th} sub-band data samples and $K_p = \sum_{b=0}^{p-1} Q_b$. At the receiver, unlike CP-OFDM, the UPMC uses the complete symbol duration of samples. Therefore, the received UPMC symbol is padded with a sufficient number of zeros for processing through 2N-point FFT. After execution of the 2N-point FFT, the even subcarriers were extracted for data detection (down sampled by a factor of 2).

3. ADAPTIVE SUB-BAND FILTER DESIGN

As we know that the FIR filtering operations provide less OBE and robustness in a relaxed synchronized system. But the filtering operation disrupts the orthogonality between the sub-carriers and causes interference. In general, the PRB-based sub-band filtering is most preferable to implemented in the UPMC waveform. In the case of multi-user and multi-services, there is design flexibility in the UPMC waveform to allocate multiple PRBs such that each service support multiple users, and one or more consecutive PRBs can be allocated to each

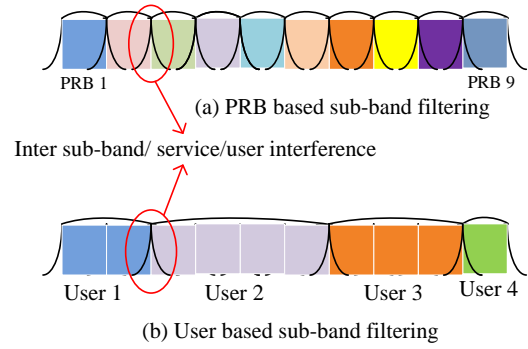


Figure 2. Types of sub-band filtering

user as shown in Figure 2. The inter-symbol interference (ISI) can be minimized by sub-band filtering operation in the UPMC system, but it might be causing some significant ISBI in the case of multi-service or multi-user systems. On the other hand, for the non-adjacent sub-bands/services, the ISBI is insignificant and does not affect the system performance.

3. 1. Interference in the UPMC Symbol As stated earlier, non-orthogonality brought on by filtering operations may cause interference between nearby subcarriers and sub-bands. To analyze the interference, let us define the ISBI and ICI in terms of desired data symbols and sub-band filter metrics. Consider the following assumptions for formulation and simplification:

Assumption 1. The modulated data symbols mapping on subcarriers are uncorrelated with each other, and have zero mean (i.e., $E[S_p(k)] = 0$ and variance $E[|S_p(k)|^2] = \sigma_{s_p}^2$

Assumption 2. The sub-band filter coefficients are normalized to have $\sum_{l=0}^{L_f-1} |f_p(l)|^2 = 1$

Consider the energy of the UPMC symbol given as follows:

$$E_{UPMC} = \sum_{n=0}^{N+L_f-2} |x(n)|^2 \quad (5)$$

The energy of the UPMC symbol can be expressed as:

$$E_{UPMC} = \sum_{n=0}^{N+L_f-2} x(n) x^*(n) = \sum_{n=0}^{N+L_f-2} (\sum_{p=0}^{B-1} x_p(n)) (\sum_{q=0}^{B-1} x_q^*(n)) = E_{SB} + E_{ISBI} \quad (6)$$

where $x^*(n)$ represents the complex conjugative of $x(n)$. By substituting Equation (1) in Equation (9), the UPMC symbol energy can be composed of two components, one is the total sub-band energy (E_{SB}) for $p = q$ and another one is the ISBI component (E_{ISBI}) for $p \neq q$. These energy components can be expressed as:

$$E_{SB} = \sum_{p=q=0}^{B-1} \sum_{n=0}^{N+L_f-2} |x_p(n)|^2 = \sum_{n=0}^{N+L_f-2} \sum_{p=0}^{B-1} \sum_{l=0}^{L_f-1} |f_p(l)|^2 R_{s_p, s_p} \quad (7)$$

$$E_{ISBI} = \sum_{n=0}^{N+L_f-2} \sum_{p=0}^{B-1} \sum_{q=0}^{B-1} x_p(n) x_q^*(n) = \sum_{n=0}^{N+L_f-2} \sum_{p=0}^{B-1} \sum_{q=0}^{B-1} \sum_{l=0}^{L_f-1} f_p(l) f_q^*(l) R_{s_p, s_q} \quad (8)$$

where, R_{s_p, s_q} is the correlation sequence of the two different time-domain sub-band data sequence $s_p(n)$ and $s_q(n)$, which can be defined as $R_{s_p, s_q} = s_p(n-l) s_q^*(n-l)$. By substituting Equation (3) here, we get:

$$R_{s_p, s_q} = \frac{1}{N^2} \sum_{k=m=0}^{\min(Q_p, Q_q)} S_p(k) S_q^*(k) e^{j\frac{2\pi}{N}(K_p - K_q)(n-l)} + \frac{1}{N^2} \sum_{k=0}^{Q_p-1} \sum_{m=0}^{Q_q-1} S_p(k) S_q^*(m) e^{j\frac{2\pi}{N}(K_p - K_q + k - m)(n-l)} \quad (9)$$

$$R_{s_p, s_q} = \frac{1}{N^2} e^{j\frac{2\pi}{N}(K_p - K_q)(n-l)} \left(\sum_{k=0}^{\min(Q_p, Q_q)} S_p(k) S_q^*(k) + \sum_{k=0}^{Q_p-1} \sum_{m=0}^{Q_q-1} S_p(k) S_q^*(m) e^{j\frac{2\pi}{N}(k-m)(n-l)} \right) \quad (10)$$

Since the modulated data sequences (frequency-domain data sequences) are uncorrelated or low correlated for $p \neq q$ and $k \neq m$. Therefore, neglecting the second term in Equation (10) we have:

$$R_{s_p, s_q} = \frac{1}{N^2} e^{j\frac{2\pi}{N}(K_p - K_q)(n-l)} \sum_{k=0}^{\min(Q_p, Q_q)} S_p(k) S_q^*(k) \quad (11)$$

For $p = q$ the Equation (11) can be written as:

$$E_{ICI} = \frac{1}{N^2} \sum_{p=0}^{B-1} \sum_{k=0}^{Q_p-1} \sum_{m=0}^{Q_p-1} S_p(k) S_p^*(m) \sum_{n=0}^{N+L_f-2} e^{j\frac{2\pi}{N}(k-m)n} E_{f_p}(k, m) \quad (17)$$

where

$$E_{f_p}(k, m) = \sum_{l=0}^{L_f-1} |f_p(l)|^2 e^{-j\frac{2\pi}{N}(k-m)l} \quad (18)$$

$$E_{ISBI} = \frac{1}{N^2} \sum_{p=0}^{B-1} \sum_{q=0}^{B-1} \sum_{l=0}^{L_f-1} |f(l)|^2 e^{-j\frac{2\pi}{N}(\frac{Q_p - Q_q}{2})l} \sum_{n=0}^{N+L_f-2} e^{j\frac{2\pi}{N}(K_p - K_q)n} \sum_{k=0}^{\min(Q_p, Q_q)} S_p(k) S_q^*(k) \quad (19)$$

According to Equations (17) and (19), the size of the sub-band and the sub-band filter ramps have an impact on both ICI and ISBI. The filter ramps depend on the filter length, which is usually recommended to choose more than the channel length (CP length) to mitigate the multipath channel dispersion. The multipath channel effects may be partially mitigated by the filter ramp-up and ramp-down, but ISI cannot be fully removed. The sub-band filter length decides the level of non-orthogonality factor between subcarriers, the OBE, and hence the interference (ISBI and ICI). To maintain a low degree of interference, the sub-band filter order is adjusted in this article for the sub-band size. In other

$$R_{s_p, s_p} = \frac{1}{N^2} \left(\sum_{k=0}^{Q_p-1} |S_p(k)|^2 + \sum_{k=0}^{Q_p-1} \sum_{m=0}^{Q_q-1} S_p(k) S_p^*(m) e^{j\frac{2\pi}{N}(k-m)(n-l)} \right) \quad (12)$$

From (3), we have:

$$f_p(l) f_q^*(l) = |f(l)|^2 e^{j\frac{2\pi}{N}(K_p - K_q + \frac{Q_p - Q_q}{2})l} \quad (13)$$

Substitute Equation (12) in Equation (7), the total sub-band energy can be written as:

$$E_{SB} = \sum_{n=0}^{N+L_f-2} \sum_{p=0}^{B-1} \sum_{l=0}^{L_f-1} |f_p(l)|^2 \frac{1}{N^2} \left(\sum_{k=0}^{Q_p-1} |S_p(k)|^2 + \sum_{k=0}^{Q_p-1} \sum_{m=0}^{Q_q-1} S_p(k) S_p^*(m) e^{j\frac{2\pi}{N}(k-m)(n-l)} \right) \quad (14)$$

According to Equation (14), the total sub-band energy E_{SB} can be divided into two components: the sub-carrier energy (E_{SC}) component for $k = m$ and the ICI component (E_{ICI}) for $k \neq m$. Therefore, the complete UPMC symbol energy becomes:

$$E_{UPMC} = E_{SC} + E_{ICI} + E_{ISBI} \quad (15)$$

From Assumption 2 and $N \gg L_f$, the total desired data subcarriers energy of the UPMC symbol is given as:

$$E_{SC} = \frac{1}{N^2} \sum_{n=0}^{N+L_f-2} \sum_{p=0}^{B-1} \sum_{l=0}^{L_f-1} |f_p(l)|^2 \sum_{k=0}^{Q_p-1} |S_p(k)|^2 = \frac{N+L_f-1}{N^2} \sum_{p=0}^{B-1} \sum_{k=0}^{Q_p-1} |S_p(k)|^2 \quad (16)$$

and

Substituting Equations (12) and (14) in Equation (9), the inter-sub-band interference energy can be written as:

words, depending on the sub-band width, the filter length or tail in the symbol duration can be adjustable. Therefore, the filter length design is an important part of the UPMC system. In the following subsection, we focus on the filter length selection according to the sub-band size.

3. 2. Filter Length Design for Sub-band Filter

The sub-band filter design flexibility is one of the most significant advantages of the UPMC waveform compared to others, which enables to adjustment of the sub-band filtering configuration according to the requirement of service, user, and channel conditions. The Gibb's

phenomenon states that the magnitude response of the filter exhibits nearly the same oscillatory behavior (i.e., ripples) after a limited value of its order. From this vantage point, we suggested an approach that modifies the FIR filter order about sub-band size, while maintaining a minimum level of OBE. In general, tolerance schemes have been used to build filter design algorithms because they give a close approximation of the ideal filter frequency response. The FIR filter design depends on the following parameters: passband (f_p) and stopband edge frequencies (f_s), maximum absolute errors known as ripples in the passband and stopband (δ_p and δ_s) and filter length (L). The sub-band filter length (L) [31] is defined approximately as:

$$L = \frac{-10 \log(\delta_p \delta_s) - 13}{14.36 \Delta f} + 1 \quad (20)$$

where Δf represents the normalized transition width, which is defined as the difference between stopband edge frequency and passband edge frequency. i.e., $\Delta f = \frac{(f_s - f_p)}{F_s}$. The passband and stopband edge frequencies can be defined based on the bandwidth requirements of the sub-band/ service. The bandwidth (BW) of the filter is defined from the number of subcarriers allocated to the sub-band as $BW = Q f_{sc}$, where f_{sc} is the subcarrier spacing, typically an integer multiple of 15 kHz according to the 5G NR numerology. The lower (f_l) and upper (f_h) passband edge frequencies of the sub-band are defined as:

$$f_l = K_0 f_{sc} \text{ and } f_h = (K_0 + Q_p) f_{sc} \quad (21)$$

Here the stopband frequency is determined from the general filter assumption, i.e., half of the sampling frequency $\frac{F_s}{2}$ or the guard band between the sub-band or service bands i.e., $f_s = \frac{N}{2} f_{sc}$ and $\Delta f = \frac{1}{2} - \frac{K_0 + Q_p}{N}$. Substitute Δf in Equation (20), we get:

$$L = \frac{N(-10 \log(\delta_p \delta_s) - 13)}{7.18(N - K_0 - Q_p)} \quad (22)$$

The sub-band filter length decides the level of non-orthogonality factor between subcarriers, the OBE, and hence the interference (ISBI and ICI). In this paper, the sub-band FIR filter order is adapted for the sub-band size as mentioned in Equation (22) to maintain a minimum level of interference. That is the filter length or tail in the symbol duration due to filtering operation can be flexible based on the sub-band width.

4. SIMULATION RESULTS AND DISCUSSION

From the discussion in Section 3, the system performance is affected by the sub-band filter design for a given width of the sub-band in different ways. In this section, the

performance of the proposed method is evaluated through MATLAB simulation under various scenarios. To demonstrate the results clearly without sacrificing their generality, we adopted the 3GPP bandwidth configuration/ radio frame structure, i.e., the channel bandwidth of 10 MHz, 15 kHz subcarrier spacing, 624 data subcarriers, and the IFFT length $N = 1024$ for all simulation results. Let consider two different cases with different sub-band sizes ($Q = 12$ SCs and 36 SCs with 5 sub-bands) as shown in Figure 3. The first case depicted in Figure 3(a), here the sub-band ramps (i.e., OBE) due to filtering operation extended to more than one sub-band for smaller sub-band size (Q), and the power distribution among the subcarriers in a sub-band is approximately equal. This results in less frequency selectivity and there is a high likelihood of accurate data detection in the sub-band with a higher signal-to-interference ratio (SIR). In the second case (i.e., for larger sub-band sizes) shown in Figure 3(b), the ramp spread is less than one adjacent sub-band with a fixed filter length and ineffective power distribution along the subcarriers in a sub-band. Which leads to greater frequency selectivity and reduced performance.

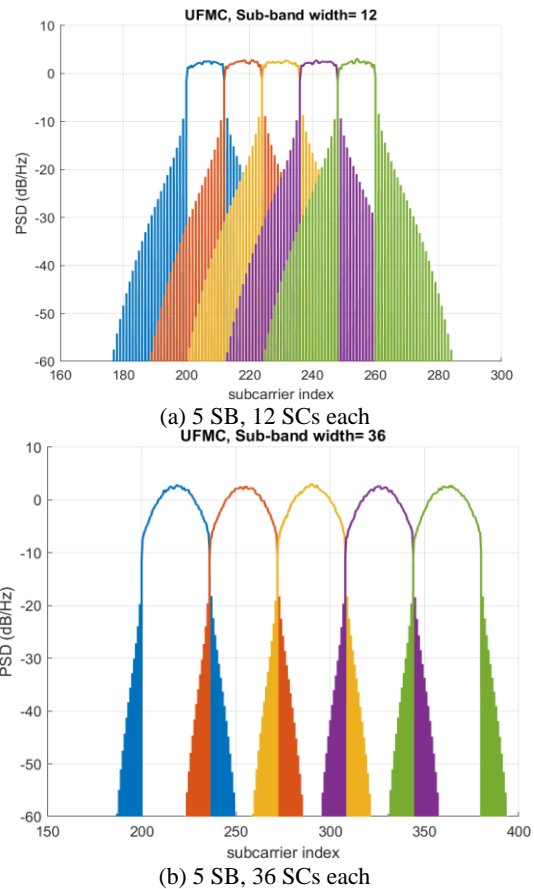


Figure 3. Power spectral density of the UPMC signal with the following specifications: 64-QAM, filter length (L_f) = 73, and $N = 1024$

The maximum to minimum filter gain ratio (MMFGR) can be used to define the frequency selectivity of the sub-band response shown in Figure 4. It is clear from Figure 4, for a fixed sub-band size, the MMFGR increases with filter length and for a fixed filter length, the MMFGR increase with sub-band width. The UFMC system with a longer filter length results in a larger MMFGR (i.e., non-uniform power allocation among the subcarriers within a sub-band and higher at the middle of the sub-band) and higher frequency selectivity, but it leads to a high possibility of error at the edges of the sub-band and causes a greater overall performance loss in terms of SNR. The higher value of MMFGR may also be impact on the best pilot pattern design to estimate channel impulse response and frequency offset error. Pilots should be assigned to the subcarriers with the highest filter gain (i.e., in the middle of one sub-band). This may increase the complexity of estimation algorithms at the receiver.

For instance, to obtain a specific MMFGR for a particular total number of subcarriers and filter length, we can choose the suitable sub-band bandwidth. Similarly, it is simple to calculate the corresponding MMFGR for a particular filter length and sub-band bandwidth, which can be used to assess the performance loss. To maintain a minimum level of MMFGR, here the filter length is adapted according to the allocated bandwidth of sub-bands and analyzed the variation of the interference with respect to filter length and sub-band width.

Figure 5 shows the variation of ISBI and ICI for simulation parameters (adopt from the 3GPP band configuration of 10 MHz bandwidth with 15 kHz subcarrier spacing) shown in Table 1. The simulation results from Figure 5 states that the cumulative ISBI decreases with the filter length due to lower OBE, and the ICI increases with filter length due to a higher level of non-orthogonality. In case of both uniform and non-uniform subcarrier allocation, the ISBI decreases, and

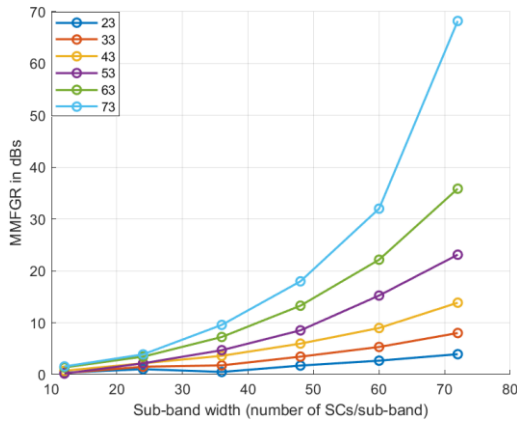


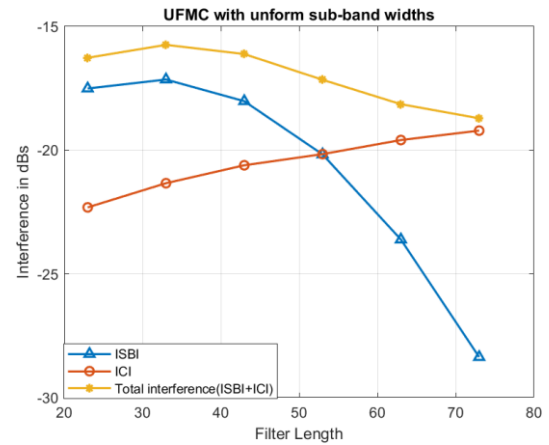
Figure 4. MMFGR variation according to the filter length and sub-band width

ICI increases with the filter length. There is a tradeoff between the interference and the filter length (i.e., the ISBI dominates for a smaller filter length and the ICI dominates for a longer filter length. To reduce this effect the sub-band filter length is dynamically modified with sub-band size to minimize the overall interference in the UFMC symbol according to Equation (22).

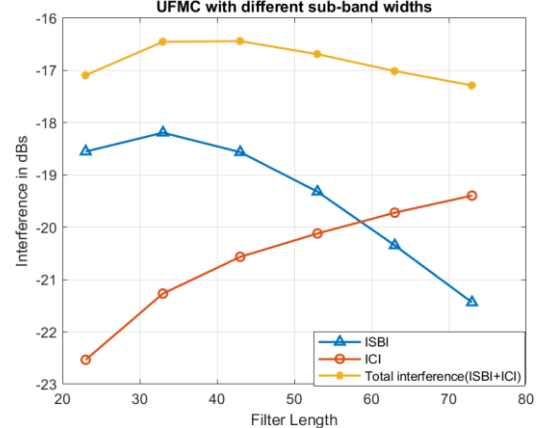
Figure 6 simulation results show how average ISBI and ICI vary for sub-band sizes of 12, 36, 48, 72, and 96 with fixed and adaptive filter lengths. From this, we

TABLE 1. Simulation parameters

| Parameter Name | Value |
|-------------------------|--|
| IFFT size (N) | 1024 |
| Modulation order | 64 QAM |
| Stopband attenuation | 40 dB |
| Sub-band size (Q) | Integer multiple of 12 SC |
| Filter length (L_f) | 73 for conventional Variable for proposed |
| Wireless channel model | Rayleigh fading |



(a) uniform subabd-width allocation



(b) non-uniform subabd-width allocation

Figure 5. Interference variation in the UFMC symbol

concluded that the proposed model is superior in terms of ISBI/ICI compared to the conventional UFGM system. With the proposed adaptive filter approach, the total interference (ICI+ISBI) is reduced by around 1.5 to 3 dB than the conventional method as shown in Figure 6(b). Furthermore, the proposed approach gives a better signal-to-interference ratio (SIR) compared to the conventional one as shown in Figure 7. The inclusion of the filter and the unequal power distribution to various subcarriers lead the average BER performance of the UFGM system in one sub-band to be worse than that of the OFDM system. This is because a frequency-selective filter responds more favorably in the middle of the sub-band than at the subcarriers on its edges as shown in Figure 3. As a result, there is a high likelihood of inaccurate detection at the edges, and the response at intermediate subcarriers may occasionally be excessively high.

Figure 8 illustrates the BER performance comparison between proposed and conventional method for the simulation parameters mentioned in Table 1. With the proposed method the filter length selection is based on the sub-band width, and the filter length values are 11, 13 and 15 for the sub-band widths of 12 ,36 and 60 SCs respectively. These values are shorter than the fixed filter length (i.e., 73) approach hence the symbol utilization improved with the proposed method as shown in Table 2.

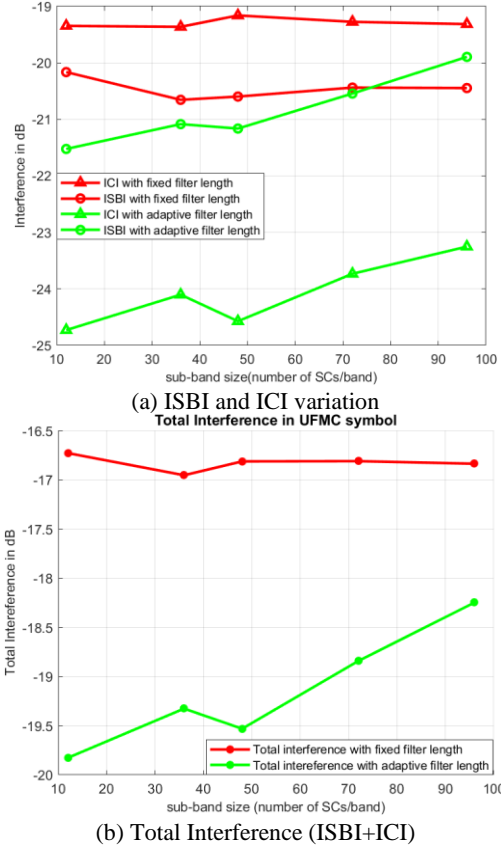


Figure 6. Interference variation with sub-band size

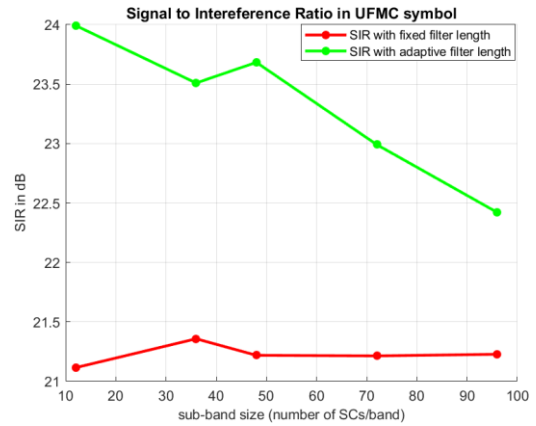


Figure 7. Signal to Interference Ratio versus sub-band size

TABLE 2. Conventional (fixed filter length) versus proposed (adaptive filter length) model

| | BW (MHz)/ f _{sc} (kHz) | Data SCs/ IFFT size N | CP length | Filter length | Tail due to filtering |
|---------------------|---------------------------------|-----------------------|-----------|---------------|-----------------------|
| Subcarrier per band | | | | 12 36 60 | |
| Conventional [12] | 10/ 15 | 624/ 1024 | 72 | 73 | 72 |
| | 100/60 | 1200/ 2048 | 144 | 145 | 144 |
| Proposed | 10/ 15 | 624/1024 | 72 | 11 13 15 | 10 to 14 |
| | 100/60 | 1200/2048 | 144 | 9 11 11 | 8 to 10 |

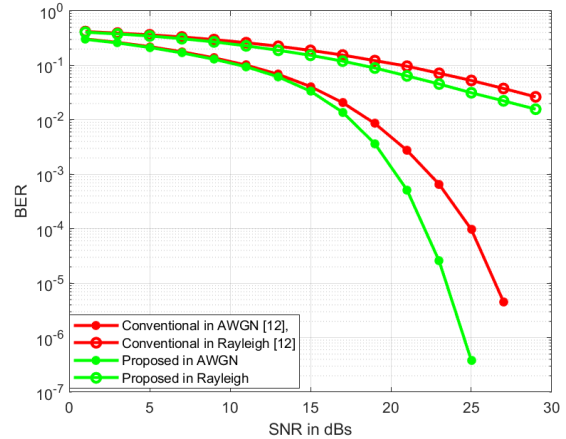


Figure 8. The UFGM system performance

By proposed method, the total interference contributed from ISBI and ICI is less than the conventional fixed filter length method results in improved SIR and hence improved the average BER performance of the system shown in Figure 8. Here, we can observe that the system attained the acceptable BER of 10⁻³ at around 21 dB and 23 dB with proposed and conventional methods, respectively. Finally, the overall simulation results

indicate that the proposed adaptive filter is appropriate for the UFMC system with multi-services.

5. CONCLUSION

The sub-band filtering process may affect the system performance in different ways directly. It is necessary to consider every subcarrier within the sub-band when selecting a filter to achieve a particular performance. Here is an idea for simplifying the filter length choice process in terms of filter response metrics. The filter length is dynamically modified to minimize interference with sub-band width. The resultant filter length obtained from the proposed method is shorter than the conventional fixed length approach. As a result, the SIR improved by 1 to 3 dBs thus improving the BER performance of the UFMC system. The computational complexity due to the filtering operation can be further reduced by applying the machine learning algorithms, this is the future scope of this work in progress.

6. REFERENCES

- Zhang, P., Li, L., Niu, K., Li, Y., Lu, G. and Wang, Z., "An intelligent wireless transmission toward 6g", *Intelligent and Converged Networks*, Vol. 2, No. 3, (2021), 244-257. doi: 10.23919/ICN.2021.0017.
- Matthaiou, M., Yurduseven, O., Ngo, H.Q., Morales-Jimenez, D., Cotton, S.L. and Fusco, V.F., "The road to 6g: Ten physical layer challenges for communications engineers", *IEEE Communications Magazine*, Vol. 59, No. 1, (2021), 64-69. doi: 10.1109/MCOM.001.2000208.
- Yang, P., Xiao, Y., Xiao, M. and Li, S., "6g wireless communications: Vision and potential techniques", *IEEE Network*, Vol. 33, No. 4, (2019), 70-75. doi: 10.1109/MNET.2019.1800418.
- Singh, S., "Environmental energy harvesting techniques to power standalone iot-equipped sensor and its application in 5g communication", *Emerging Science Journal*, Vol. 4, (2020), 116-126. doi: 10.28991/esj-2021-SP1-08.
- Wunder, G., Jung, P., Kasparick, M., Wild, T., Schaich, F., Chen, Y., Ten Brink, S., Gaspar, I., Michailow, N. and Festag, A., "5gnow: Non-orthogonal, asynchronous waveforms for future mobile applications", *IEEE Communications Magazine*, Vol. 52, No. 2, (2014), 97-105. doi: 10.1109/MCOM.2014.6736749.
- Farhang-Boroujeny, B., "Filter bank multicarrier modulation: A waveform candidate for 5g and beyond", *Advances in Electrical Engineering*, Vol. 2014, (2014). doi: 10.1155/2014/482805.
- Banelli, P., Buzzi, S., Colavolpe, G., Modenini, A., Rusek, F. and Ugolini, A., "Modulation formats and waveforms for 5g networks: Who will be the heir of ofdm?: An overview of alternative modulation schemes for improved spectral efficiency", *IEEE Signal Processing Magazine*, Vol. 31, No. 6, (2014), 80-93. doi: 10.1109/MSP.2014.2337391.
- Elkourdi, M., Peköz, B., Güvenkaya, E. and Arslan, H., "Waveform design principles for 5g and beyond", in 2016 IEEE 17th annual wireless and microwave technology conference (WAMICON), IEEE., (2016), 1-6.
- Demir, A.F., Elkourdi, M., Ibrahim, M. and Arslan, H., "Waveform design for 5g and beyond", arXiv preprint arXiv:1902.05999, (2019).
- Fettweis, G., Krondorf, M. and Bittner, S., "Gfdm-generalized frequency division multiplexing", in VTC Spring 2009-IEEE 69th Vehicular Technology Conference, IEEE., (2009), 1-4.
- Nissel, R., Schwarz, S. and Rupp, M., "Filter bank multicarrier modulation schemes for future mobile communications", *IEEE Journal on Selected Areas in Communications*, Vol. 35, No. 8, (2017), 1768-1782. doi: 10.1109/JSAC.2017.2710022.
- Zhang, L., Ijaz, A., Xiao, P., Molu, M.M. and Tafazolli, R., "Filtered ofdm systems, algorithms, and performance analysis for 5g and beyond", *IEEE Transactions on Communications*, Vol. 66, No. 3, (2017), 1205-1218. doi: 10.1109/TCOMM.2017.2771242.
- Vakilian, V., Wild, T., Schaich, F., ten Brink, S. and Frigon, J.-F., "Universal-filtered multi-carrier technique for wireless systems beyond lte", in 2013 IEEE Globecom Workshops (GC Wkshps), IEEE., (2013), 223-228.
- Schaich, F. and Wild, T., "Waveform contenders for 5g—ofdm vs. Fbmc vs. Ufmc", in 2014 6th international symposium on communications, control and signal processing (ISCCSP), IEEE., (2014), 457-460.
- Schaich, F., Wild, T. and Chen, Y., "Waveform contenders for 5g-suitability for short packet and low latency transmissions", in 2014 IEEE 79th Vehicular Technology Conference (VTC Spring), IEEE., (2014), 1-5.
- Zhang, L., Ijaz, A., Xiao, P. and Tafazolli, R., "Multi-service system: An enabler of flexible 5g air interface", *IEEE Communications Magazine*, Vol. 55, No. 10, (2017), 152-159. doi: 10.1109/MCOM.2017.1600916.
- Zhang, L., Ijaz, A., Xiao, P., Quddus, A. and Tafazolli, R., "Subband filtered multi-carrier systems for multi-service wireless communications", *IEEE Transactions on Wireless Communications*, Vol. 16, No. 3, (2017), 1893-1907. doi: 10.1109/TWC.2017.2656904.
- Lin, T.-T. and Chen, T.-C., "Complexity-reduced receiver for universal filtered multicarrier systems", *IEEE Wireless Communications Letters*, Vol. 8, No. 6, (2019), 1667-1670. doi: 10.1109/LWC.2019.2935191.
- Manda, R. and Gowri, R., "Universal filtered multicarrier receiver complexity reduction to orthogonal frequency division multiplexing receiver", *International Journal of Engineering, Transactions A: Basics*, Vol. 35, No. 4, (2022), 725-731. doi: 10.5829/ije.2022.35.04A.12.
- Saad, M., Al-Ghouwayel, A. and Hijazi, H., "Ufmc transceiver complexity reduction", in 2018 25th International Conference on Telecommunications (ICT), IEEE., (2018), 295-301.
- Nadal, J., Nour, C.A. and Baghdadi, A., "Novel uf-ofdm transmitter: Significant complexity reduction without signal approximation", *IEEE Transactions on Vehicular Technology*, Vol. 67, No. 3, (2017), 2141-2154. doi: 10.1109/TVT.2017.2764379.
- Matthé, M., Zhang, D., Schaich, F., Wild, T., Ahmed, R. and Fettweis, G., "A reduced complexity time-domain transmitter for uf-ofdm", in 2016 IEEE 83rd Vehicular Technology Conference (VTC Spring), IEEE., (2016), 1-5.
- Mukherjee, M., Shu, L., Kumar, V., Kumar, P. and Matam, R., "Reduced out-of-band radiation-based filter optimization for ufmc systems in 5g", in 2015 international wireless communications and mobile computing conference (IWCMC), IEEE., (2015), 1150-1155.
- Zhang, Z., Wang, H., Yu, G., Zhang, Y. and Wang, X., "Universal filtered multi-carrier transmission with adaptive active interference cancellation", *IEEE Transactions on*

- Communications*, Vol. 65, No. 6, (2017), 2554-2567. doi: 10.1109/TCOMM.2017.2681668.
25. Chen, X., Wu, L., Zhang, Z., Dang, J. and Wang, J., "Adaptive modulation and filter configuration in universal filtered multi-carrier systems", *IEEE Transactions on Wireless Communications*, Vol. 17, No. 3, (2017), 1869-1881. doi: 10.1109/TWC.2017.2786231.
 26. Wen, J., Hua, J., Lu, W., Zhang, Y. and Wang, D., "Design of waveform shaping filter in the ufmc system", *IEEE Access*, Vol. 6, (2018), 32300-32309. doi: 10.1109/ACCESS.2018.2837693.
 27. Yarrabothu, R.S. and Nelakuditi, U.R., "Optimization of out-of-band emission using kaiser-bessel filter for ufmc in 5g cellular communications", *China Communications*, Vol. 16, No. 8, (2019), 15-23. doi: 10.23919/JCC.2019.08.002.
 28. Zhang, L., Ijaz, A., Xiao, P., Wang, K., Qiao, D. and Imran, M.A., "Optimal filter length and zero padding length design for universal filtered multi-carrier (UFMC) system", *IEEE Access*, Vol. 7, (2019), 21687-21701. doi: 10.1109/ACCESS.2019.2898322.
 29. Manda, R. and Gowri, R., "Filter design for universal filtered multicarrier (UFMC) based systems", in 2019 4th International Conference on Information Systems and Computer Networks (ISCON), IEEE. (2019), 520-523.
 30. Wang, X., Wild, T. and Schaich, F., "Filter optimization for carrier-frequency-and timing-offset in universal filtered multi-carrier systems", in 2015 IEEE 81st Vehicular Technology Conference (VTC Spring), IEEE. (2015), 1-6.
 31. Rabiner, L.R., McClellan, J.H. and Parks, T.W., "Fir digital filter design techniques using weighted chebyshev approximation", *Proceedings of the IEEE*, Vol. 63, No. 4, (1975), 595-610. doi: 10.1109/PROC.1975.9794.

COPYRIGHTS

©2023 The author(s). This is an open access article distributed under the terms of the Creative Commons Attribution (CC BY 4.0), which permits unrestricted use, distribution, and reproduction in any medium, as long as the original authors and source are cited. No permission is required from the authors or the publishers.



Persian Abstract

چکیده

شبکه های بی سیم آینده از Universal Filtered Multicarrier (UFMC) به عنوان یک تکنیک مدولاسیون شکل موج جدید استفاده خواهند کرد. شکل موج UFMC به طور معقولی مشخصات فیلتر زیر باند مانند ترتیب فیلتر و شکل را در نظر می گیرد تا مزایای کلیدی شکل موج های مدولاسیون نسل فعلی را ترکیب کند و در عین حال از معایب آنها جلوگیری کند. بنابراین در سیستم های مبتنی بر UFMC توجه به نحوه ساخت فیلتر فرعی حائز اهمیت است. در این مقاله، پیکربندی فیلتر زیر باند با توجه به اندازه زیر باند تطبیق داده شده است به طوری که نماد UFMC حداقل سطح تداخل را با حداقل انتخاب فرکانس ایجاد می کند. همچنین کل تداخل ناشی از تداخل بین حامل (ICI) و تداخل بین زیر باند (ISBI) با یافتن شکل بسته تغییر آن در سیگنال UFMC با اندازه زیر باند و طول فیلتر مورد بررسی قرار گرفت. از این تجزیه و تحلیل، ما تعیین کردیم که ICI با طول فیلتر افزایش و ISBI کاهش می یابد. بنابراین، روش پیشنهادی طول فیلتر را از نظر اندازه زیر باند و تداخل بهینه می کند. با این روش، طول فیلتر کمتر از روش معمولی است و از این رو استفاده از نماد را بهبود می بخشد. با روش پیشنهادی، نسبت کلی سیگنال به تداخل (SIR) بین ۱ تا ۳ دسی بل بهبود یافت.